



FT-IR and FT-Raman study of Nasicon type phosphates, $\text{ASnFe}(\text{PO}_4)_3$ [A = Na₂, Ca, Cd]

C.J. Antony^a, A. Aatiq^b, C. Yohannan Panicker^{c,1}, M. Junaid Bushiri^{d,*}, Hema Tresa Varghese^{e,1}, T.K. Manojkumar^f

^a Department of Science and Humanities, Kingston Engineering College, Vellore, Tamilnadu 632059, India

^b Department de chimie, Laboratoire de Chimie des Matériaux Solides, Casablanca, Morocco

^c Department of Physics, TKM College of Arts and Science, Kollam, Kerala, 691005 India

^d Department of Physics, Cochin University of Science and Technology, Cochin, Kerala, 682022 India

^e Department of Physics, Fatima Mata National College, Kollam, Kerala, 691001 India

^f Indian Institute of Information Technology and Management – Kerala, Technopark, Thiruvananthapuram, India

ARTICLE INFO

Article history:

Received 8 March 2010

Received in revised form 27 October 2010

Accepted 15 November 2010

Keywords:

FT-Raman

FT-IR

Nasicon

Phosphates

ABSTRACT

FT-Raman and FT-IR spectra of $\text{ASnFe}(\text{PO}_4)_3$ [A = Na₂, Ca, Cd] were recorded and analyzed. The bands were assigned in terms of the vibrational group frequencies of SnO₆ octahedral and PO₄ tetrahedral. The spectral analysis shows that the symmetry of corner shared octahedral (SnO₆) and the tetrahedral (PO₄) are lowered from their free ion symmetry state. The presence of Fe³⁺ ions disrupts the S–N–O–S–N chain in the structure. This causes distortion of SnO₆ and PO₄ in the structure of all the compounds. Also it is seen that there are two distinct PO₄ tetrahedra of different P–O bond lengths. One of these tetrahedra is linearly distorted in all the title compounds. The PO₄ frequencies and bond lengths are calculated theoretically and are in agreement with the experimental values. The presence of PO₄ polyanion in the structure can reduce the redox energy and hence reduce the metal oxygen covalency strength in the structure.

© 2010 Elsevier B.V. All rights reserved.

1. Introduction

Nasicon-type materials have been extensively studied as solid electrolytes, ionic conductors, electrode materials, low thermal expansion ceramics, sensors, etc. [1–3]. Jrifi et al. [4] reported the preparation, structural characterization and spectroscopic studies of Nasicon type arsenate. Phosphates within the Nasicon-type family have been the subject of intensive research due to their potential application as a solid electrolyte, electrode material and low thermal expansion ceramics [5–10]. These materials are having general formula $\text{A}_x\text{BB}'(\text{PO}_4)_3$ and crystallizes into rhombohedral $R\bar{3}C(D_{3d}^6)$ structure in which (B)'BO₆ octahedra shares corners with PO₄ tetrahedra. Within the Nasicon type structure, there are inter connected interstitial sites M1 (one per formula unit) and M2 (three per formula unit) between which the cation A can diffuse causing fast ion conductivity [7,10]. The choice of transition metal has a significant effect on the cell voltage as it primarily depends on the

redox couple of the metal atom present in the structure [8,11]. Phosphates within the Nasicon type structure containing elements like Ti, Nb, Sn, V, etc. are important due to the fact that these elements have more than one oxidation state [7]. Ionic conductivity of these compounds can be enhanced by the substitution of tetravalent elements like Ti with trivalent elements like Al, Fe, etc. [8,11]. The iron based phosphates are relatively economic and environmentally friendly ones [11]. The structure of $\text{ASnFe}(\text{PO}_4)_3$ [A = Na₂, Ca, Cd] is determined with the help of powder diffraction data and Rietveld refinement [7]. The analysis of vibrational spectra of these compounds can provide vital information on covalency strength and hence to understand its efficiency for battery applications [8]. The present study aims to investigate the internal structures of the title compounds by analyzing the Raman and FT-IR spectra.

2. Experimental

Nasicon type phosphates $\text{ASnFe}(\text{PO}_4)_3$ [A = Na₂, Ca, Cd] used in the present study were synthesized by the conventional solid state reaction technique [7]. Mixtures of carbonate ACO_3 [A = Na₂, Ca, Cd], oxides SnO₂ and Fe₂O₃ and phosphate $\text{NH}_4\text{H}_2\text{PO}_4$ were taken in stoichiometric proportion for the solid-state reaction. The heated product after the reaction gives powder crystalline samples [7]. Raman spectra (Fig. 1) of the compounds were

* Corresponding author. Tel.: +91 9895370968.

E-mail addresses: cyphyp@rediffmail.com (M.J. Bushiri), h.varghese@rediffmail.com (H.T. Varghese).

¹ Temporary address: Research Centre, Department of Physics, Mar Ivanios College, Trivandrum, Kerala, India.

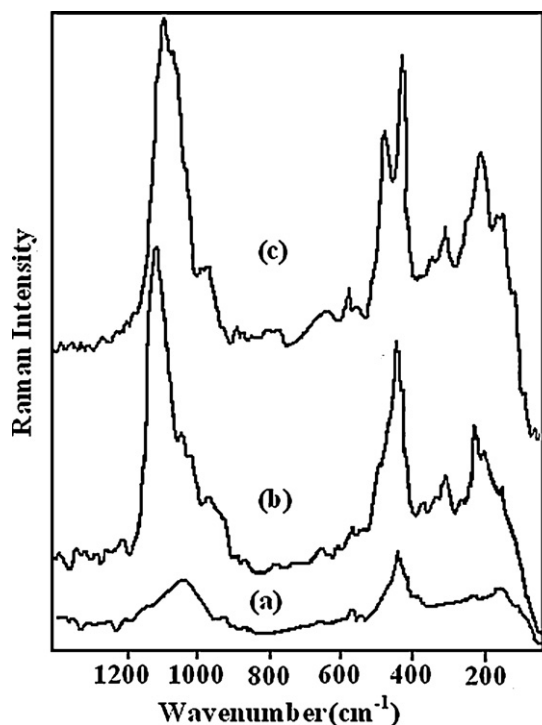


Fig. 1. Raman spectra of (a) $\text{Na}_2\text{SnFe}(\text{PO}_4)_3$ (b) $\text{CaSnFe}(\text{PO}_4)_3$ and (c) $\text{CdSnFe}(\text{PO}_4)_3$.

recorded by using Bruker FT-Raman spectrometer in the Stokes region ($50\text{--}4000\text{ cm}^{-1}$). The FT-IR spectra (Fig. 2) were recorded by using Bruker IFS-66v-FTIR spectrometer in the spectral region of $400\text{--}4000\text{ cm}^{-1}$ using KBr pellet method.

3. Factor group analysis

All the title compounds $\text{ASnFe}(\text{PO}_4)_3$ [$A = \text{Na}, \text{Ca}, \text{Cd}$] abbreviated as NaSF, CaSF and CdSF respectively crystallise in the hexagonal system with space group $R\bar{3}C(D_{3d}^5)$ with $Z = 6$ and $Z^B = 2$ [7]. In NaSF, the sodium atoms, four in number occupy the C_3 site, the Fe and Sn atoms two each in number occupy respectively the sites C_{3i} and D_3 . All the six P atoms are accommodated in the C_2 site whereas the 24 oxygen atoms to the general site C_1 . In $\text{ASnFe}(\text{PO}_4)_3$ [$A = \text{Ca}, \text{Cd}$], the A atom two in number is in the D_3 site, whereas the Fe and Sn atoms, two each are occupying respectively the C_{3i} and C_i sites. All the six phosphate atoms are in the C_2 site. The general site C_1 accommodates 24 oxygen atoms. The vibrational

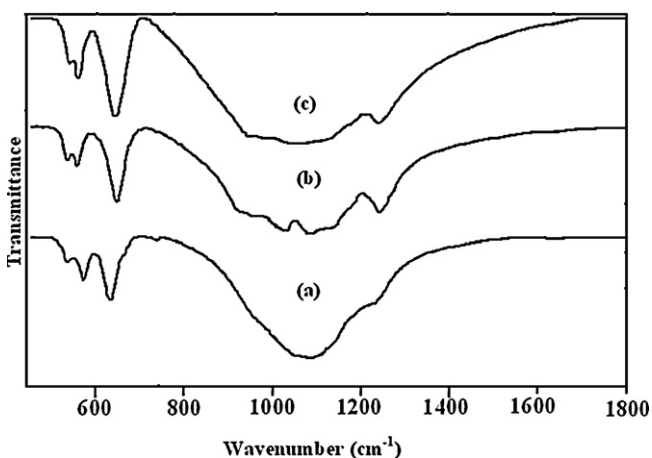


Fig. 2. FT-IR spectra of (a) $\text{Na}_2\text{SnFe}(\text{PO}_4)_3$ (b) $\text{CaSnFe}(\text{PO}_4)_3$ and (c) $\text{CdSnFe}(\text{PO}_4)_3$.

modes of these compounds were obtained by the group theoretical method by Fateley et al. [12]. The total irreducible representations excluding the acoustic modes are distributed as (Tables 1 and 2).

1. For NaSF $\begin{cases} 111 = 11A_{1g} + 13A_{2g} + 15E_g + 12A_{1u} + 13A_{2u} + 16E_u \\ 105 = 10A_{1g} + 12A_{2g} + 13E_g + 12A_{1u} + 13A_{2u} + 16E_u \end{cases}$
2. For CaSF $\begin{cases} 105 = 10A_{1g} + 12A_{2g} + 13E_g + 12A_{1u} + 13A_{2u} + 16E_u \\ 105 = 10A_{1g} + 12A_{2g} + 13E_g + 12A_{1u} + 13A_{2u} + 16E_u \end{cases}$
3. For CdSF $\begin{cases} 105 = 10A_{1g} + 12A_{2g} + 13E_g + 12A_{1u} + 13A_{2u} + 16E_u \\ 105 = 10A_{1g} + 12A_{2g} + 13E_g + 12A_{1u} + 13A_{2u} + 16E_u \end{cases}$

4. Results and discussion

The Raman and FT-IR spectra of the title compound were analyzed in terms of the vibrational frequencies of SnO_6 octahedra and PO_4 tetrahedra. The spectral band assignments are given in Table 3.

4.1. Vibrational analysis

The structure of the NaSF belongs to the Nasicon type structure in which the structural frame work is built up by corner shared octahedra $\text{Sn}(\text{Fe})\text{O}_6$ and tetrahedra PO_4 . In this framework, each octahedron is surrounded by six tetrahedra and each tetrahedron by four octahedra. There are four interconnected cation sites usually labeled as M1 (one per formula unit) and M2 (three per formula unit) which can be represented by the crystallographic $[\text{M}2]_3[\text{M}1]\text{BB}'(\text{PO}_4)_3$ formula. The occupancy of the cation in the M1 or M2 sites depends mainly on the nature and the number of A atoms in the compound and on the nature of the BB' elements within the Nasicon structure. In NaSF the Na^+ ions are distributed in the M1 and M2 sites with one atom each and the $\text{Sn}^{4+}(\text{Fe}^{3+})$ are randomly distributed [7]. The structural refinement suggests that Fe^{3+} ions are occupying the Sn^{4+} ion sites and hence the possibility of different Fe/Sn–O bonds. Hence the SnO_6 octahedra is disturbed and distorted due to the presence of Fe^{3+} ions in the site. Also it is seen that the ionic radii of Fe^{3+} and Sn^{4+} are almost equal ($r_{\text{Fe}} = 0.645\text{ \AA}$ and $r_{\text{Sn}} = 0.69\text{ \AA}$). Due to the equivalence of these ions in equivalent sites in the structure of the compound, there is the possibility of Fe^{3+} ions disrupting the Sn–O–Sn and Sn–O–P chains in the structure. The structure of CaSF and CdSF are similar to that of NaSF with slight change in occupancy of cations (Ca^{2+} and Cd^{2+}). The cations Ca^{2+} and Cd^{2+} are located in the M1 site only.

4.2. SnO_6 vibrations

$\text{Sn}(\text{Fe})\text{O}_6$ octahedra is one of the important building block in the title compounds with random distribution [7]. The SnO_6 octahedra with O_h symmetry in its free ion state has six fundamental modes of vibration similar to other metal oxygen octahedras like TiO_6 , NbO_6 , MoO_6 , etc. [13–17]. These fundamental modes are symmetric stretching mode ν_1 (A_{1g}), asymmetric stretching modes ν_2 (E_g) and ν_3 (F_{1u}), asymmetric bending mode ν_4 (F_{1u}), symmetric bending mode ν_5 (F_{2g}) and the Raman and IR inactive mode ν_6 (F_{2u}). The ν_1 , ν_2 , and ν_5 modes are Raman active, whereas the ν_3 and ν_4 modes are IR active [13]. In SnO_2 , the Sn atoms form octahedra with oxygen atoms and as a result above mentioned, fundamental modes of metal oxygen octahedra are expected. The A_{1g} mode of SnO_2 shows higher frequency as compared with TiO_2 , in spite of SnO_2 being less compact than TiO_2 . In accordance to this concept, the Raman active modes of symmetries B_{1g} and B_{2g} of SnO_2 are actually softer than the corresponding modes of TiO_2 [18]. Further, the Sn–O bond strength is expected to be lesser in the title compounds as a result of incorporation of Fe^{3+} ion into the Sn site and the Raman active modes of SnO_6 octahedra are likely to soften its intensity. In bulk SnO_2 , Raman bands are reported at 636.3 (A_{1g}) cm^{-1} as an intense one, followed by the mode B_{2g} at 780.9 cm^{-1} and the mode

Table 1 D_{3d} factor group species, translations, acoustical modes, vibrational modes and infrared and Raman activity of $A\text{SnFe}(\text{PO}_4)_3$ crystal [A = Ca, Cd].

D_{3d} space group species	Translation species	Acoustic modes	Factor group coefficients	Coefficient of vibrational species	IR/Raman activity
A_{1g}	–	–	10	10	Raman active
A_{2g}	–	–	12	12	Inactive mode
E_g	–	–	13	13	Raman active
A_{1u}	–	–	12	12	Inactive mode
A_{2u}	T_z	1	14	13	IR active
E_u	T_x, T_y	1	17	16	IR active

Table 2 D_{3d} factor group species, translations, acoustical modes, vibrational modes and infrared and Raman activity of $\text{Na}_2\text{SnFe}(\text{PO}_4)_3$ crystal.

D_{3d} space group species	Translation species	Acousted modes	Factor group coefficients	Coefficient of vibrational species	IR/Raman activity
A_{1g}	–	–	11	11	Raman active
A_{2g}	–	–	13	13	Inactive mode
E_g	–	–	15	15	Raman active
A_{1u}	–	–	12	12	Inactive mode
A_{2u}	T_z	1	14	13	IR active
E_u	T_x, T_y	1	17	16	IR active

E_g at 474.1 cm^{-1} due to vibrations of SnO_6 octahedra [19,20]. The fully symmetric A_{1g} stretching vibrations of an isolated SnO_6 give rise to A_{1g} and B_{2g} pair in the spectra. The A_{1g} and B_{2g} modes are in phase and out of phase phonons of the same vibration are along Sn–O bonds. Usually, the frequencies of these two phonons are very similar or even indistinguishable [21–23]. A comparatively weak band is observed in the Raman spectrum of CaSF at 657 cm^{-1} and its IR counterpart at 641 cm^{-1} . Similarly a weak and broad band is present in the Raman spectrum of CdSF at 629 cm^{-1} and a relatively strong band in the IR spectrum at 645 cm^{-1} . But the band in this region is absent in the Raman spectrum of NaSF. The B_{2g} mode is present as a broad band at 788 and 784 cm^{-1} in the Raman spectra of CdSF and CaSF respectively. As per the structural information, the overall set of Sn(Fe)–O distances within the framework is slightly varied in the title compounds. Sn(Fe)–O(1) is $1.953(4)\text{ \AA}$, Sn(Fe)–O(2) is $2.045(4)\text{ \AA}$ in NaSF, Sn(Fe)–O distances are 1.962 \AA and 2.062 in CdSF. The Sn(Fe)–O in CaSF is found to be 1.968 and 2.054 \AA [7]. These values show a distortion of the Sn(Fe) O_6 octahedra in these samples. A linear increase of M1–O(2) distance versus A

cation ionic radii (r_A), is observed in $\text{ASnFe}(\text{PO}_4)_3$ (A = Na_2 , Ca, Cd) phases. This will lead to the relatively higher order distortion of SnO_6 octahedra in CaSF and CdSF as compared to that of NaSF. This is evident from the activation of B_{2g} modes in the Raman spectra and A_{1g} modes in the IR spectra of CaSF and CdSF. The bands are also observed in the region corresponds to the E_g mode of SnO_6 octahedra, an unambiguous assignment of this mode is limited due to the expectation of ν_2 modes of PO_4 tetrahedra in this region. The Raman active ν_5 vibration is also stronger especially in the case of more distorted octahedral as reported in TiO_6 octahedra of KTiOPO_4 crystal [15]. Such a strong band profile is not seen in the spectra of present samples below 250 cm^{-1} , ruling out the possibility of higher order distortion of the SnO_6 octahedra. The observed bands correspond to this mode of vibrations are assigned in Table 3 [24]. The broad Raman spectral nature of $(\text{SnFe})\text{O}_6$ shows a disorder in the structure of CaSF and CdSF. The presence of Fe^{3+} ions in the equivalent sites of Sn^{4+} ions disrupts the SnO_6 octahedra, lowering its symmetry from its free ion state. Also the Sn–O–Sn and Sn–O–P chain in the structure is distorted and disrupted due to the influence of Fe^{3+} ions

Table 3Spectral data (cm^{-1}).

$\text{Na}_2\text{SnFe}(\text{PO}_4)_3$		$\text{CaSnFe}(\text{PO}_4)_3$		$\text{CdSnFe}(\text{PO}_4)_3$		Assignments
Raman	IR	Raman	IR	Raman	IR	
168 vvwa	–	145 w	–	143 w	–	Lattice modes
–	–	201 w	–	208 m	–	
220 vvw	–	226 m	–	230 sh	–	–
250 sh	–	254 sh	–	–	–	–
–	–	–	–	–	–	–
–	–	309 ms	–	302 w	–	ν_5 SnO_6
–	–	348 sh	–	318 w	–	–
–	–	380 vw	–	–	–	–
416 sh	–	–	–	425 s	–	ν_2 PO_4
449 s	–	436 s	–	–	–	–
–	–	–	–	471 m	–	ν_2 SnO_6
–	–	486 sh	–	490 sh	–	–
530 m	536 vvw	–	532 w	–	536 w	ν_4 PO_4
571 m	568 m	576 w	561 m	571 w	564 m	ν_4 PO_4
–	–	600 w	–	–	–	–
–	633 vs	657 w	641 s	629 w	645 s	ν_1 SnO_6
–	735 vvw	784 w	–	788 w	–	SnO_6 (B_{2g})
–	–	977 sh	954 sh	988sh	941 sh	ν_1 PO_4
–	–	999 sh	–	–	–	–
1042 ms	–	1046 sh	1035vvs 1041 sh	–	–	ν_3 PO_4
946–1213	1088 vs	1106 vs	1092vvs 1083 vs	–	1094vs	ν_3 PO_4
–	–	1213 w	1140vvs 1189 w	–	1142 s	ν_3 PO_4
1250 vvw	1230 sh	–	1248 s	–	–	–

vw—very weak; w—weak; sh—shoulder; ms—moderately strong; vvs—very very strong, s—strong, vs—very strong, s—strong.

in the sites of Sn^{4+} . In NaSF, metal oxygen octahedral vibrational bands are absent which is probably due to the low polarizability (Fig. 1).

4.3. Vibrations of PO_4^{3-} tetrahedra

The PO_4 tetrahedra with T_d symmetry in its free form have four fundamental modes of vibration. These modes are Raman active, but ν_3 and ν_4 modes are active in the infrared spectrum only [13–16]. The ν_1 – ν_3 modes in NaSF is observed as a broad band extending from 946 to 1213 cm^{-1} with moderately intense peak at 1042 cm^{-1} in Raman spectrum. In the IR spectrum, a broad band from 850 to 1300 cm^{-1} with a very strong peak at 1088 followed by a shoulder at 1230 cm^{-1} is appeared. Similarly broad band is observed in the Raman spectrum of CaSF from 910 to 1213 cm^{-1} with very strong intensity peak at 1106 cm^{-1} along with shoulders at 977, 999 and 1046 cm^{-1} (Fig. 1). Correspondingly, the IR spectrum gives intense peaks at 1035 and 1092 cm^{-1} with shoulders at 954 and 1140 cm^{-1} . The Raman spectrum of CdSF gives a broad band from 920 to 1189 cm^{-1} with intense peak at 1083 cm^{-1} with shoulder at 1041 cm^{-1} . But in the IR spectrum of CdSF, strong bands are observed at 1094 and 1142 cm^{-1} (Fig. 2). The P–O bond length is varied from 1.521 to 1.562 with a mean a mean distance of 1.54 Å in NaSF. This is of the order of 1.502 and 1.565 with an average distance 1.534 Å in CaSF and is having maximum variation among the compounds under investigation [7]. This variation in P–O distance is in agreement with the presence of shoulders in the Raman spectrum of CaSF at 977 and 999 cm^{-1} . In CdSF also P–O distance shows variation which is in the range 1.508–1.538 Å.

The large size cations like Na in conducting channel may leads to compression of PO_4 tetrahedra due to its relative size [25]. As a result, the PO_4 tetrahedra are expected to be more compressed in NaSF than that of CaSF and CdSF. The intramolecular PO_4^{3-} bending modes (ν_2 and ν_4) are more sensitive to conducting ion insertion than the intramolecular PO_4^{3-} stretching modes (ν_1 and ν_3) as reported in $\text{Li}_3\text{Ti}_2(\text{PO}_4)_3$ [26]. This is because ν_2 and ν_4 are less localized than ν_1 or ν_3 and are more susceptible to small structural changes in the unit cell. Usually, the doubly degenerate ν_2 mode appears at 420 cm^{-1} in regular PO_4 tetrahedra [26]. In the present study, this band is shifted towards higher wavenumber side and appeared in the Raman spectrum of NaSF at 449 cm^{-1} . In CaSF also this band is shifted in the higher frequency side and observed at 436 cm^{-1} . In CdSF, this is appeared at 425 cm^{-1} which is near to its free state value. The ionic radii of Na^{2+} , Ca^{2+} and Cd^{2+} are 1.02 Å, 1.00 Å, 0.95 Å, respectively [7]. The shifting of ν_4 mode towards higher wavenumber from its free state value is increased with increase of ionic radii of M1 ions. Thus the PO_4 tetrahedra in NaSF are more distorted than those of CaSF and CdSF.

The triply degenerate ν_4 mode appears in the Raman spectrum of NaSF at 530 and 571 cm^{-1} and its degeneracy is found to be partially lifted. In the IR spectrum also its degeneracy is partially lifted and two bands are observed at 536 and 568 cm^{-1} . Almost similar observations are noticed in the other samples also, the detailed band assignments are given in Table 3.

The appearance of ν_1 – ν_3 mode in the higher wave number region than that of its free state value suggests the linear distortion of the PO_4 tetrahedra. Splitting observed in the spectral pattern of the title compounds in the ν_3 region of PO_4 tetrahedra indicate the lifting of degeneracy of this mode and is due to the distortion [13–16]. Normally in Nasicon structure the PO_4 tetrahedra Raman bands are intense, ruling out the metal oxygen chain [27]. Broadening of the spectral band also suggests the distortion of PO_4 tetrahedra [16]. The occupation of Fe^{3+} ion

in equivalent positions of Sn in $\text{Sn}(\text{Fe})\text{O}_6$ octahedra sharing corners with PO_4 tetrahedra can also contribute disorder in PO_4 tetrahedra.

The PO_4 unit gives nine vibrational modes that are characterized by non-degenerate symmetric $\nu_s(\text{PO})$, antisymmetric triply degenerate $\nu_{as}(\text{PO})$ of phosphorous non-bridging stretching and the symmetric doubly degenerate $\delta_d(\text{OPO})$ bending [28]. Anantharamulu et al. [28] observed these in the frequency ranges 1270–1000, 1000–900, 670–540 and 450–440 cm^{-1} . In order to facilitate the analysis of the vibrational spectra, we have performed ab initio calculations of the PO_4 group theoretically using Gaussian 03 software [29] package. Internal modes involve the displacement of oxygen atoms of the tetrahedral PO_4^{3-} anions and present frequencies closely related to those of the free molecule. For PO_4^{3-} , the theoretical calculations give the frequencies as, 790, 789, 788, 730, 444, 443, 443, 309 and 308 cm^{-1} which are the symmetric and antisymmetric stretching mode of the P–O bonds and O–P–O symmetric and antisymmetric bending mode. The differences between experimental and calculated vibrational modes are observed, since the experimental results belong to solid phase and theoretical calculations belong to gaseous phase. In a solid, internal modes can split as a consequence of two effects: the site symmetry effect due to an electric crystal field of symmetry lower than the tetrahedral acting on the molecule and the correlation effect due to the presence of more than one molecular group in the crystal unit cell. According to Winand et al. [30] for condensed phosphates, the intensity of P–O stretching Raman bands near 1000 cm^{-1} are always greater than those near 740 cm^{-1} , assigned to the stretching of P–O–P bridges. Hatert [31] reported the P–O bond lengths in the range 1.533–1.538 Å and the O–P–O angles in the range 109.7–112.1° whereas in the present case the theoretical calculations give the corresponding bond lengths in the range 1.6275–1.6267 Å and the angle as 109.5°.

It is reported that the presence of polyanions like PO_4^{3-} shown to be lowering $\text{Me}^{3+}/\text{Me}^{2+}$ redox energy to useful levels in lithium cells in which Li based Nasicon phosphates are used. Polarisation of the electrons of the O^{2-} ions into strong covalent bonding within the polyanion reduces the covalent bonding to the metal ion, which lowers its redox energy [9]. Similarly in Nasicon compounds, like the title compounds the presence of PO_4^{3-} shown to lower the redox energy of $\text{Fe}^{3+}/\text{Sn}^{4+}$ couple. The weak nature of spectral profiles ascribed to metal–oxygen octahedra in the title compounds indicate that its covalency strength is weak as compared to that of PO_4^{3-} covalency strength. As a result, lower redox energy is expected from the $\text{Fe}^{3+}/\text{Sn}^{4+}$ redox couple which can give a better cell voltage. The covalency strength of PO_4^{3-} anion in CaSF and CdSF is estimated to be of the order of 0.35 and as a result, these compounds are expected to give better performance for battery applications [8]. The redox energy of the redox couple $\text{Fe}^{3+}/\text{Sn}^{4+}$ is anticipated to be less due to higher order covalency strength of PO_4^{3-} in CaSF and CdSF and low polarizability of $(\text{SnFe})\text{O}_6$ octahedra in all the title compounds.

5. Conclusion

The observed bands are assigned in terms of vibrations of PO_4 tetrahedra and SnO_6 octahedra. The SnO_6 octahedra in NaSF are having less polarizability, in CaSF and in CdSF this octahedral are disordered and distorted. The PO_4 tetrahedra are also distorted and disordered in title compounds. The PO_4 frequencies and bond lengths were calculated theoretically and the values are in agreement with the experimental values. The covalency strength of PO_4^{3-} anion in CaSF and CdSF is estimated to be of the order of 0.35, and these compounds are expected to give better performance for battery applications.

Acknowledgement

TKM is thankful for the financial support by KSCSTE, Kerala and DST, Government of India.

References

- [1] J.L. Rodrigo, P. Carrasco, J. Alamo, *Mater. Res. Bull.* 24 (1989) 611–618.
- [2] L. Brian, B.L. Cushing, J.B. Goodenough, *J. Solid State Chem.* 162 (2001) 176–181.
- [3] A. Aatiq, C. Delmas, A. El-Jazouli, *J. Solid State Chem.* 158 (2001) 169–174.
- [4] A. Jrifi, A. El-Jazouli, J.P. Chaminade, M. Couzi, *Powder Diffr.* 24 (2009) 200–204.
- [5] K.J. Rao, K.C. Sobha, S. Kumar, *Proc. Indian Acad. Sci. (Chem. Sci.)* 113 (2001) 497–514.
- [6] G. Butt, N. Sammes, G. Tompsett, A. Smirnova, O. Yamamoto, *J. Power Sources* 134 (2004) 72–79.
- [7] A. Aatiq, *Powder Diffr.* 19 (2004) 272–279.
- [8] C.M. Julien, P. Jozwiak, J. Garbarczyk, *Proceedings of the International Workshop Advanced Techniques for Energy Sources Investigation and Testing*, Sofia, Bulgaria, 2004, pp. 4–6.
- [9] S.Y. Chung, J.T. Bloking, Y.M. Chiang, *Nat. Mater.* C1 (2002) 123–128.
- [10] M.J. Bushiri, C.J. Antony, A. Aatiq, *J. Phys. Chem. Solids* 69 (2008) 1985–1989.
- [11] K.S. Nanjundaswamy, A.K. Padhi, J.B. Goodenough, S. Okada, H. Ohtsuka, H. Arai, J. Yamaki, *Solid State Ionics* 92 (1996) 1–10.
- [12] W.G. Fateley, F.R. Dollish, N.T. Mc Devitt, F.F. Bentley, *Infrared and Raman Selection Rules for Molecular and Lattice Vibrations – The Correlation Method*, Wiley, New York, 2002.
- [13] K. Nakamoto, *Infrared and Raman Spectra of Inorganic and Coordination Compounds—Part A*, 5th ed., Wiley-Interscience, New York, 1997.
- [14] M. Issac, *Investigations on the Raman and Infrared Spectra of Certain Molybdates*, Ph. D. Thesis, University of Kerala, 1992.
- [15] G.E. Kugel, F. Brehat, B. Wyncke, M.D. Fontana, G. Marnier, C. Carabatos-Nedelac, J. Mangin, *J. Phys. C: Solid State Phys.* 21 (1988) 5565–5583.
- [16] M.J. Bushiri, V.U. Nayar, *J. Nonlinear Opt. Phys. Mater.* 10 (2001) 345–353.
- [17] M.J. Bushiri, R.S. Jayasree, M. Fakhfakh, V.U. Nayar, *Mater. Chem. Phys.* 73 (2002) 179–185.
- [18] T. Hirata, K. Ishioka, M. Kitajima, H. Doi, *Phys. Rev. B* 53 (1996) 8442–8448.
- [19] Z.W. Chen, J.K.L. Lai, C.H. Shek, *Phys. Rev. B* 70 (2004) 165314–165320.
- [20] P.S. Peercy, B. Morosin, *Phys. Rev. B* 7 (1973) 2779–2786.
- [21] M.V. Abrashev, G.A. Zlateva, E. Dinolova, *Phys. Rev.* 47B (1993) 8320–8323.
- [22] A. de Andres, S. Taboada, J.L. Martinez, A. Salinas, J. Hernandez, R. Saez-Puche, *Phys. Rev.* 47B (1993) 14898–14904.
- [23] E.J. Flynn, S.A. Solin, G.N. Papatheodorou, *Phys. Rev.* 13 B (1976) 1752–1758.
- [24] A.M. Heyns, P.M. Harden, *J. Phys. Chem. Solids* 60 (1999) 277–284.
- [25] K.B.R. Varma, K.V.R. Prasad, *J. Phys. D: Appl. Phys.* 23 (1990) 1723–1726.
- [26] C.M. Burba, R. Frech, *Solid State Ionics* 177 (2006) 1489–1494.
- [27] C.E. Bamberger, G.M. Begun, O.B. Cavin, *J. Solid State Chem.* 73 (1988) 317–324.
- [28] N. Anantharamulu, G. Prasad, M. Vithal, *Bull. Mater. Sci.* 31 (2008) 133–138.
- [29] M.J. Frisch, G.W. Trucks, H.B. Schlegel, G.E. Scuseria, M.A. Robb, J.R. Cheeseman, J.A. Montgomery, Jr., T. Vreven, K.N. Kudin, J.C. Burant, J.M. Millam, S.S. Iyengar, J. Tomasi, V. Barone, B. Mennucci, M. Cossi, G. Scalmani, N. Rega, G.A. Petersson, H. Nakatsuji, M. Hada, M. Ehara, K. Toyota, R. Fukuda, J. Hasegawa, M. Ishida, T. Nakajima, Y. Honda, O. Kitao, H. Nakai, M. Klene, X. Li, J.E. Knox, H.P. Hratchian, J.B. Cross, C. Adamo, J. Jaramillo, R. Gomperts, R.E. Stratmann, O. Yazyev, A.J. Austin, R. Cammi, C. Pomelli, J.W. Ochterski, P.Y. Ayala, K. Morokuma, G.A. Voth, P. Salvador, J.J. Dannenberg, V.G. Zakrzewski, S. Dapprich, A.D. Daniels, M.C. Strain, O. Farkas, D.K. Malick, A.D. Rabuck, K. Raghavachari, J.B. Foresman, J.V. Ortiz, Q. Cui, A.G. Baboul, S. Clifford, J. Cioslowski, B.B. Stefanov, G. Liu, A. Liashenko, P. Piskorz, I. Komaromi, R.L. Martin, D.J. Fox, T. Keith, M.A. Al-Laham, C.Y. Peng, A. Nanayakkara, M. Challacombe, P.M. W. Gill, B. Johnson, W. Chen, M.W. Wong, C. Gonzalez, J.A. Pople, *Gaussian 03, Revision C.02*, Gaussian: Wallingford, 2004.
- [30] J.M. Winand, A. Rulmont, P. Tarte, *Solid State. Chem.* 93 (1991) 341–349.
- [31] F. Hatert, *Acta Cryst.* E65 (2009) i30.